ELSEVIER

Journal of Chromatography B, 783 (2003) 181–190

JOURNAL OF CHROMATOGRAPHY B

www.elsevier.com/locate/chromb

Simultaneous quantitative determination method for ceramide species from crude cellular extracts by high-performance liquid chromatography–thermospray mass spectrometry

Mototeru Yamane*

Department of Biochemistry, Tokyo Medical University, 6-1-1 Shinjuku, Shinjuku-ku, Tokyo 160, Japan

Received 26 March 2002; received in revised form 1 August 2002; accepted 26 August 2002

Abstract

I have developed a simple method which enabled simultaneous analysis of ceramides in the subcellular fractions from cultured cells by HPLC–thermospray mass spectrometry. The HPLC–thermospray mass spectra from ceramide standards were characterized by the high intensity of the MNa^+ and $MH^+–H_2O$ ions. As the other minor ions, MK^+, MH^+ and *m*/*z* 282 ions were detected. Although the preponderance of MNa^+ ions compared with the $MH^+–H_2O$ ions was detected in non-hydroxy fatty acid-ceramides, the preponderance of $MH^+–H_2O$ ions based on the elimination of the hydroxyl group introduced at the α-position of acyl-portion compared with the MNa^+ ions was detected in α-hydroxy fatty acid-ceramides. In calibrations for authentic ceramides using *N*-octanoylsphingosine as an internal standard, an approximately linear relationship existed between the ratios of peak-areas of each ceramide to that of the internal standard and the known amounts of each ceramide. The factor (*f*) of each ceramide was calculated as follows; *N*-oleoyl-D-sphingosine (*f*=0.45), *N*-palmitoyl-D-sphingosine (*f*=0.40), *N*-stearoyl-D-sphingosine (*f*=0.39), *N*-nervonoyl-D-sphingosine (*f*=0.39) and *N*-lignoceroyl-D-sphingosine (*f*=0.35). In subcellular fractions from A549 and HepG2 cells, although ceramide species content per mg protein was high in the nuclear envelope fractions, the 7000 *g* pellet fractions and the 100 000 *g* pellet fractions, a large portion of the ceramide species was concentrated in the nuclear envelope fraction. In addition, this method was applied to a mild alkaline hydrolyzate of total ceramides from pig stratum corneum, and $MNa^+/MH^+–H_2O$ ions corresponding to several ω-hydroxyacyl-ceramides were detected.

Keywords: Nuclear envelope fraction; Ceramide

1. Introduction

Ceramides (CERs) have recently been identified as key signaling molecules which mediate many biological functions [1] such as cell growth [2], differentiation [3,4], senescence [5] and apoptosis [6]. Simple, sensitive and accurate methods for ceramide quantification are needed in view of their biological importance. A variety of different techniques are used for CER measurement. Up until now, the diacylglycerol (DAG) kinase assay has been the most commonly used procedure for CER quantitation in the range of 25 to 2000 pmol [7]. However, this assay does not allow for identification and quantification of individual ceramide species and the spe-

*Fax: +81-3-3739-9945.

E-mail address: m-yamane@tokyo-med.ac.jp (M. Yamane).

1570-0232/02/$ – see front matter
PII: S1570-0232(02)00637-2

cificity of this assay has recently been questioned by a report comparing the DAG kinase assay with a mass spectrometry (MS) method [8]. Alternative methods include a variety of procedures which use thin-layer chromatography (TLC) [9–12] or high-performance liquid chromatography (HPLC) with prior derivatization steps [13–16]. Recently, MS methodologies have been developed for detection of CERs which use atmospheric pressure chemical ionization (APCI) MS or electrospray ionization (ESI) MS/ESI-tandem MS [17–21,28].

Thermospray (TSP) ionization has been widely used as a stable interface for HPLC–MS for 10 years. This interface has low running costs because essential nebulizing gas as in APCI and ESI is not needed. However, since TSP ionization was believed to be unsuitable for ionization of a nonpolar compound such as CER, a report of a detection method of CER using HPLC–TSP-MS analysis was not found. While the intensities of NH_4^+ ion (m/z 18) and CH_3-OH-NH_4^+ ion (m/z 50) from a nonpolar mobile phase in HPLC–TSP-MS, in fact, were low, the intensities of base ions from the solutes such as CERs were relatively high. In the present study, I first established a simple method which enabled simultaneous analysis of CERs in the subcellular fractions from cultured cells by HPLC–TSP-MS.

2. Experimental

2.1. Materials and lipid standards

D-Erythro-sphingosine (D-sphingosine, d18:1), *N*-palmitoyl-D-sphingosine (d18:1-C16:0-CER), *N*-stearoyl-D-sphingosine (d18:1-C18:0-CER), *N*-oleoyl-D-sphingosine (d18:1-C18:1-CER), *N*-lignoceroyl-D-sphingosine (d18:1-C24:0-CER), *N*-nervonoyl-D-sphingosine (d18:1-C24:1-CER) and α-hydroxy fatty acid ceramides from bovine brain were obtained from Sigma–Aldrich (Deisenhofen, Germany), *N*-octanoylsphingosine (d18:1-C8:0-CER), *N*-octanoylsphinganine (d18:0-C8:0-CER), D-erythro-dihydrosphingosine (D-sphinganine, d18:0) and threo-phytosphingosine (t18:0) were from Biomol Research Labs. (Plymouth Meeting, PA, USA). Solvents for HPLC–TSP-MS and lipid extraction were of analytical grade from Wako (Osaka, Japan).

2.2. Cell culture

HepG2 and A549 cells (ATCC, Rockville, MD, USA) were grown in 75 cm^2 flasks containing Git medium [Daigo's T medium containing 3151 mg/l glucose and 10% cow serum growth factor (Daiogo GF-21); Nihon Pharmaceutical, Osaka, Japan] at 37 °C in a 5% CO_2 incubator.

2.3. Pig stratum corneum

Pig skins or human epidermal cysts were obtained at a slaughter house or from surgical operation. Pig stratum corneum was prepared as previously described by Wertz and Downing [22].

2.4. Sample preparation of the subcellular fractions from cultured cells

To prepare the subcellular fractions, HepG2 or A549 cells were grown for 7 or 11 days after subculture and fractionated by differential centrifugation as described previously [23]. HepG2 cells were removed from three 75 cm^2 flasks, washed and then homogenized with a Potter–Elvehjem PTFE homogenizer in 2.0 ml of 250 m*M* sucrose–50 m*M* KCl–2 m*M* $MgCl_2$–20 m*M* Tris–HCl isoosmolaric buffer (pH 7.6). A549 cells were removed from a 75 cm^2 flask, washed and homogenized with a Polytron homogenizer in 2.0 ml of the isoosmolaric buffer. Each fraction of homogenate, nuclear envelope, 7000 *g* pellet, 100 000 *g* pellet or 100 000 *g* supernatant was collected. A 200-μl aliquot of the homogenate was transferred to a glass tube with a glass stopper. The nuclear envelope fraction was suspended with a Polytron homogenizer in 2.0 ml of the isoosmolaric buffer and 0.5 or 1.0 ml of the suspension was transferred to the glass tube. Each of the 7000 *g* pellet or 100 000 *g* pellet was treated with ultrasonic waves for 20 s in 0.25 ml of 8.5 g/l NaCl and 0.2 ml of the suspension was transferred to the glass tube. A 10-μl aliquot of each suspension was assayed with the BCA Protein Assay Kit from Pierce (Rockford, IL, USA). Each of the samples in the glass tube were diluted to 1.0 ml with water, 2.0 ml of methanol (CH_3OH) was added and treated with ultrasonic waves for 30 s. To each of the suspensions, 1.0 ml (containing 11.74 nmol of d18:1-C8:0-CER) of chlo-

roform ($CHCl_3$) solution containing 11.74 μ*M* of d18:1-C8:0-CER as an internal standard was added, and the mixture was shaken for 1 min. To the suspension, 1 ml of water and 1 ml of $CHCl_3$ were added, and the mixture was shaken for 30 s. The mixture was centrifuged at 600 *g* for 5 min. The lower layer was transferred to a glass tube. The extraction of the upper layer was repeated twice using 2 ml of $CHCl_3$. The collected $CHCl_3$ solution was evaporated to dryness under reduced pressure. The residue was dissolved in 1.0 ml of CH_3OH–$CHCl_3$ (1:2, v/v) and applied to a Sep-Pak silica cartridge (Waters, Milford, MA, USA) equilibrated with CH_3OH–$CHCl_3$ (1:19, v/v). The samples were eluted with 6 ml of CH_3OH–$CHCl_3$ (1:19, v/v), and all the eluent was collected in a glass tube. The collected solution was evaporated to dryness under reduced pressure. The residue (total CER fraction) was dissolved in 100 μl of CH_3OH–$CHCl_3$ (1:1, v/v) and 20-μl aliquots were examined with the HPLC–TSP-MS system.

2.5. CER extraction from pig stratum corneum

Pig stratum corneum was successively extracted with CH_3OH–$CHCl_3$ (1:2), (1:1) and (2:1) (v/v) as previously described by Wertz and Downing [22]. The combined extracts were filtered through a No. 5A filter paper (Toyo Roshi Kaisha, Tokyo, Japan) and evaporated to dryness under reduced pressure. Total CER fractions in the residue were fractionated with a Sep-Pak silica cartridge as described above, and the concentrations of total CER fractions were examined with HPLC–TSP-MS.

2.6. ω-Hydroxyacyl CER from pig stratum corneum

Total CERs from pig stratum corneum were subjected to mild alkaline hydrolysis with 1.0 ml of 1 *M* NaOH in 90% CH_3OH at 37 °C for 1 h as described previously [22,24]. A 2-ml volume of $CHCl_3$ was then added and the mixture was shaken for 15 min. The mixture was then shaken with 4.5 ml of water and then centrifuged at 600 *g* for 5 min. The lower ($CHCl_3$) layer was then separated, washed two times with 3 ml of water, and evaporated to dryness under reduced pressure. The residue was dissolved in 200 μl of CH_3OH–$CHCl_3$ (1:1, v/v) and then 20-μl aliquots were examined with HPLC–TSP-MS.

2.7. HPLC–TSP-MS

A Shimadzu (Kyoto, Japan) LC–MS quadrupole (QP) 1000S mounted on an QP mass spectrometer, equipped with a Vestec (Houston, TX, USA) Model 750B HPLC–TSP-MS interface, a Shimadzu LC-9A HPLC pump and a Rheodyne injector, fitted with a 20-μl loop, was used. Reversed-phase HPLC separation was carried out on a Pegasil-C_8 column (100×4.6 mm I.D., Senshu Scientific, Tokyo, Japan), with a mobile phase of 0.05 *M* ammonium formate–CH_3OH solution for measurement of CERs or 0.1 *M* ammonium formate–0.1 *M* formic acid–acetonitrile (4:1:28.3, v/v) for measurement of sphingoid base at a flow-rate of 1.0 ml/min. The TSP interface temperature was optimized for maximum detection sensitivity. In the positive ion mode, the optimal vaporizer control, vaporizer tip, vapor, block and tip heater temperatures were maintained at 133, 206, 295, 326 and 334 °C, respectively, under the electron beam (filament)-off condition.

2.8. Calibration lines for CER measurement

For calibration line measurement, a known amount of each authentic CER (d18:1-C16:0-CER, d18:1-C18:0-CER, d18:1-C18:1-CER, d18:1-C24:0-CER or d18:1-C24:1-CER) and 11.74 nmol 18:1-C8:0-CER as internal standard were mixed and examined with HPLC–TSP-MS as described above.

2.9. Long-chain bases from CERs

The eluent corresponding to each CER species in the HPLC–TSP mass chromatogram from total CER fraction in the nuclear envelope fraction of cultured cells was collected by a change of HPLC–TSP-MS flow-line to a drain and evaporated to dryness under reduced pressure. Authentic CERs or the cellular CERs were hydrolyzed by reflux in 4.0 ml of 1 *M* KOH–CH_3OH solution at 75 °C for 20 h. To the hydrolysate, 4 ml of diethyl ether and 4 ml of water were added. The mixture was shaken for 1 min. The upper layer was transferred to a glass tube and evaporated to dryness under reduced pressure. The

residue was dissolved in 100 μl of ethanol and then 20-μl aliquots were examined with HPLC–TSP-MS as described above.

3. Results and discussion

The HPLC–TSP mass spectra produced from CER standards were characterized by the high intensity of the MNa^+ and $MH^+–H_2O$ ions as shown in Fig. 1A and B. Although a preponderance of MNa^+ ions compared with the $MH^+–H_2O$ ions was detected in non-hydroxy fatty acid ceramides (see Scheme 1 for CER fragmentation pattern), a preponderance of $MH^+–H_2O$ ions compared with the MNa^+ ions was detected in α-hydroxy fatty acid ceramides. It is thought that $MH^+–H_2O$ ion from α-hydroxy fatty acid CER is made of the sum of $MH^+–H_2O$ ion based on the elimination of the hydroxyl group introduced at the α-position of acyl-portion and

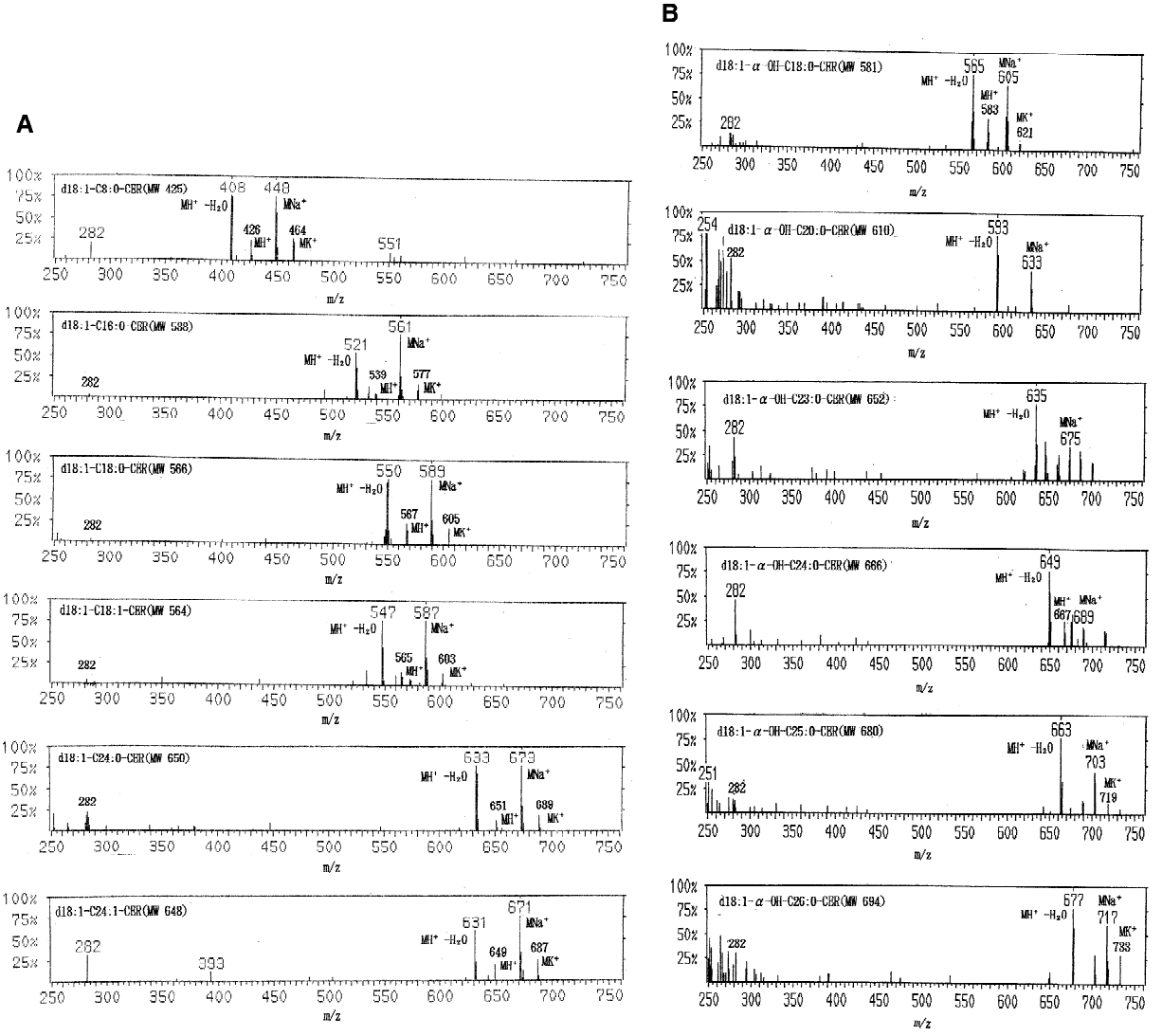

Fig. 1. HPLC–TSP mass spectra obtained from non-hydroxy fatty acid CERs and α-hydroxy fatty acid CERs. HPLC and TSP conditions as described in Experimental. Scan speed, 1.0 scan/s from *m*/*z* 250 to 750. Filament off condition. (A) Non-hydroxy fatty acid CERs; (B) α-hydroxy fatty acid CERs.

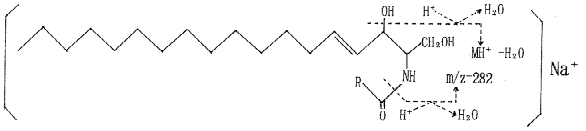

Scheme 1. CER fragmentation pattern.

$MH^+–H_2O$ ion as shown in Scheme 1. As the other minor ions, MK^+, MH^+ and m/z 282 ions were detected. The m/z 282 ion was assigned to a fragment ion corresponding to loss of a water molecule and loss of the fatty acid side chain of CER (Scheme 1), but additional analysis was not performed. The m/z 282 ion corresponded to the $MH^+–H_2O$ from d18:1 as described below.

Since the Na^+ ion is brought as common contaminants of the mobile phase solvent from glass products and the atmosphere rather than the impurity in the sample, a complete exclusion of Na^+ ion from the experimental system is very difficult and thus the utilization of the Na^+ adduct ion for the identification has been recommended. Reproducibility of the peak-area ratios of base ions in HPLC–TSP-MS analysis [selected-ion monitoring (SIM) chromato-

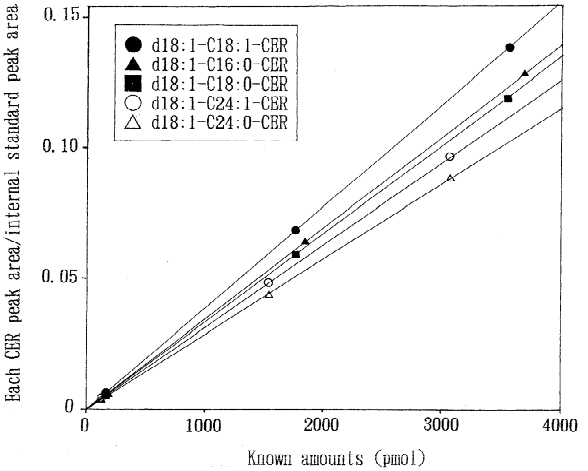

Fig. 2. Calibration lines for authentic CERs. The sum of the peak-area corresponding to each CER on each SIM chromatogram of $MNa^+/MH^+–H_2O$ ions was compared with the sum of the peak-area corresponding to d18:1-C8:0-CER as the internal standard on each SIM chromatogram of MNa^+ (m/z 448) and $MH^+–H_2O$ (m/z 408), and the ratios of peak-areas of each CER to that of the internal standard were calculated. The factor (f) of each CER was calculated as follows; d18:1-C18:1-CER ($f=0.45$), d18:1-C16:0 ($f=0.40$), d18:1-C18:0 ($f=0.39$), d18:1-C24:1-CER ($f=0.36$) and d18:1-C2 4:0-CER ($f=0.35$).

Table 1
Reproducibility of the peak-area ratios of base ions in HPLC–TSP-MS analysis (SIM chromatogram) of CERs on different days

CER	Peak-area ratio of the base ions (%)					
	MK^+	MNa^+	MH^+	$MNH_4^+–H_2O$	$MH^+–H_2O$	$MNa^+ + MH^+–H_2O$
d18:0-C8:0-CER[a]	5.16±0.43	58.22±2.61	3.59±0.55	19.85±1.38	13.14±1.33	71.37±1.67
d18:1-C24:0-CER[b]	12.68±1.41	66.45±1.39	0.50±0.15	1.08±0.27	19.15±1.29	85.60±1.57
d18:1-C24:1-CER[b]	10.52±2.43	61.70±6.73	1.96±1.17	4.07±2.42	21.70±3.89	83.41±.65

The displayed values are mean±S.D. of the peak-area ratios (%) from 9[a] or 7[b] different days.

Table 2
Comparison of APCI, ESI and TSP ionization in d18:1-CER/d18:0-CER

Ionization	CER	Cone voltage (V)	Comparative merits of base ion intensities	Nebulizing gas	Refs.
APCI	d18:1-CER	15	$MH^+ > MH^+–H_2O >> MNa^+$	+	[17]
		30	$MH^+–H_2O >> m/z$ 264		
		45	m/z 264		
	d18:0-CER	15	MH^+		
		30	MH^+		
		45	m/z 266		
ESI	d18:1-CER	14	$MH^+ > MH^+–H_2O$	+	[18,28]
	d18:0-CER	14	$MH^+ > MH^+–H_2O$		
TSP	d18:1-CER	–	$MNa^+ > MH^+–H_2O > MK^+$	–	This report
	d18:0-CER	–	$MNa^+ > MNH_4^+–H_2O \fallingdotseq MH^+–H_2O > MK^+$		

gram] of CER standards at the different days is shown in Table 1. Since good reproducibility of the MNa^+ or $MH^+–H_2O$ ion was obtained for the d18:1-CERs, the sum of the peak-areas of MNa^+ and $MH^+–H_2O$ ions was utilized in HPLC–TSP-MS analysis of the d18:1-CERs as described below. The comparison with APCI, ESI and TSP ionization is shown in Table 2. The production of the Na^+ adduct ion as MNa^+ ion in HPLC–MS was a marked tendency with successive, TSP, APCI, and ESI ionizations. Thus, in the quantitative analysis of d18:1-CERs, the sum of the peak-areas from MH^+/$MH^+–H_2O$ ion was utilized in ESI-MS analysis [20,28] and the sum of the peak-areas from MNa^+/$MH^+–H_2O$ ion was utilized in TSP-MS analysis.

The calibration lines for authentic CERs are shown in Fig. 2. The sum of the peak-areas corresponding to each CER on each SIM chromatogram of MNa^+ and $MH^+–H_2O$ ions was compared with the sum of the peak-areas corresponding to d18:1-C8:0-CER as the internal standard on each SIM chromatogram of MNa^+ (m/z 448) and $MH^+–H_2O$ (m/z 408), and the ratios of peak-areas of each CER to that of the internal standard were calculated. An approximately linear relationship existed between the ratios and the known amounts of each CER in the range of 15 to 3700 pmol (Fig. 2). The factor (f) of each CER was calculated as follows; d18:1-C18:1-CER ($f=0.45$), d18:1-C16:0-CER ($f=0.40$), d18:1-C18:0-CER ($f=0.39$), d18:1-C24:1-CER ($f=0.36$) and d18:1-C24:0-CER ($f=0.35$).

The SIM chromatograms of MNa^+ and $MH^+–$

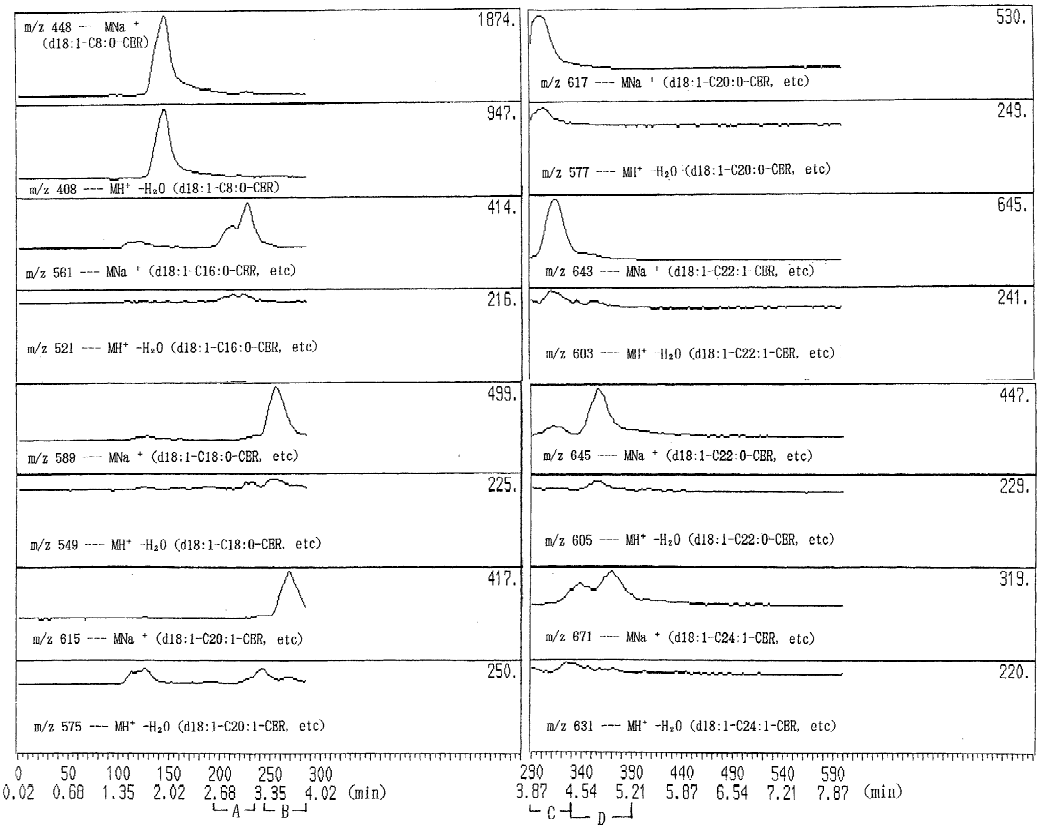

Fig. 3. SIM chromatograms of MNa^+ and $MH^+–H_2O$ ions from total CERs in the nuclear envelope fraction of A549 cells. A 0.05 *M* ammonium formate–methanol solution was used as the mobile phase. Other conditions were as described in Experimental. Filament off condition. The number in the upper right-hand corner of each chromatogram is the ion-count. The eluent (A–D) corresponding to each CER species in the chromatogram was collected by a change of HPLC–TSP-MS flow-line to a drain and evaporated to dryness under reduced pressure.

H_2O ions from the total CER fraction in the nuclear envelope fraction of A549 cells are shown in Fig. 3. The eluent corresponding to each CER species in the chromatogram of Fig. 3 was collected and the CER contents were hydrolyzed. The HPLC–TSP mass spectra produced from d18:1, d18:0 and t18:0 standards, and the SIM chromatograms of the long-chain bases from the hydrolysates are shown in Figs. 4 and 5. The mass spectra of d18:1, d18:0 and t18:0 standards were characterized by the high intensity of MNa^+ and MH^+ ions as shown in Fig. 4A, B and C. As the other minor ion from d18:1, $MH^+–H_2O$ (m/z 282) ion was detected (Fig. 4A). The peaks of MNa^+/MH^+ ions corresponding to d17:1, d18:1, d19:1 and d20:1 on the SIM chromatograms of the CER-hydrolysate from the nuclear envelope fraction were detected as shown in Fig. 5, although the peaks corresponding to d18:0, t18:0, d21:1 and d22:1 were not detectable. The hydrolysate from the eluent corresponding to fraction A in the chromatogram of Fig. 3 contained d17:1, d18:1, d19:1, d20:1 at a ratio of 4.9:9.2:1.0:1.7; fraction B contained a ratio of 5.4:2.3:1.0:0.9; fraction C contained a ratio of 2.7:3.8:1.0:1.2; and fraction D a ratio of

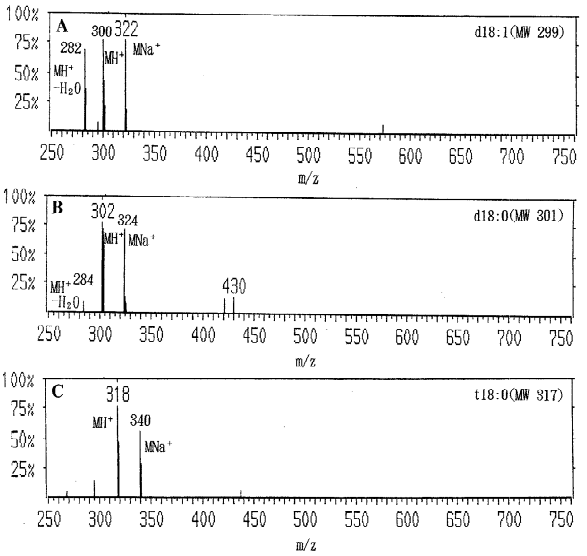

Fig. 4. HPLC–TSP mass spectra obtained from d18:1, d18:0 and t18:0 standards. HPLC and TSP conditions were as described in Experimental. Scan speed, 1.0 scan/s from m/z 250 to 750. Filament off condition. (A) d18:1; (B) d18:0; (C) t18:0.

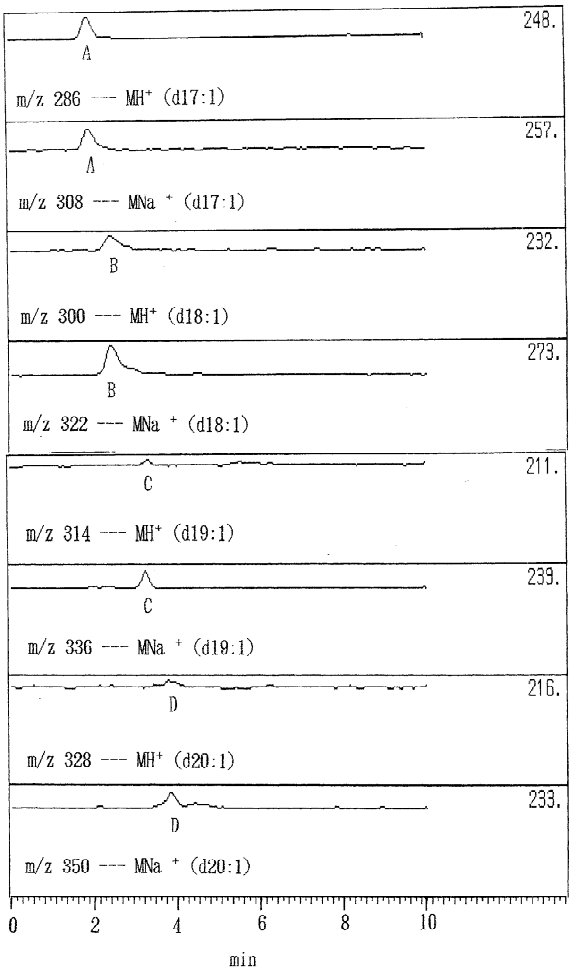

Fig. 5. SIM chromatograms of MNa^+ and MH^+ ions corresponding to each long-chain base from the hydrolysate of the fraction corresponding to each CER species from the nuclear envelope fraction of A549 cells. A 0.1 *M* ammonium formate–0.1 *M* formic acid–acetonitrile (4:1:28.3, v/v) solution was used as the mobile phase. The number in the upper right-hand corner of each chromatogram is the ion-count. (Peak A) d17:1; (peak B) d18:1; (peak C) d19:1; (peak D) d20:1.

2.9:8.3:1.0:2.1. Consequently, fraction A would likely consist of d18:1-C16:0-CER, d17:1-C17:0-CER, d20:1-C14:0-CER and d19:1-C15:0-CER in order of the content. Similarly, fraction B would likely consist of d17:1-C19:0-CER/d17:1-C21:1-CER, d18:1-C18:0-CER/d18:1-C20:1-CER, d19:1-C17:0-CER/d19:1-C19:1-CER and d20:1-C16:0-CER/d20:1-C18:1-CER; fraction C would likely consist of

Table 3
Subcellular localization of each CER content in A549 cells

Fraction	d18:1-C16:0-CER (pmol/mg protein)	Yield (%)	d18:1-C18:0-CER (pmol/mg protein)	Yield (%)	d18:1-C20:1-CER (pmol/mg protein)	Yield (%)	d18:1-C20:0-CER (pmol/mg protein)	Yield (%)	d18:1-C22:1-CER (pmol/mg protein)	Yield (%)	d18:1-C22:0-CER (pmol/mg protein)	Yield (%)	d18:1-C24:1-CER (pmol/mg protein)	Yield (%)
Homogenate	639±125[a]	100[b]	1837±374[a]	100[b]	1266±206[a]	100[b]	2058±166[a]	100[b]	1645±245[a]	100[b]	661±82[a]	100[b]	899±342[a]	100[b]
Nuclear envelope	3161±853[a]	54[b]	7024±1954[a]	26[b]	4953±893[a]	34[b]	7132±2068[a]	31[b]	4530±1036[a]	40[b]	2899±932[a]	42[b]	3878±947[a]	49[b]
7000 *g* pellet	2007±467[a]	8[b]	5717±503[a]	7[b]	3175±240[a]	7[b]	6124±697[a]	7[b]	5584±631[a]	7[b]	2604±357[a]	9[b]	3171±451[a]	11[b]
100 000 *g* pellet	1333±349[a]	7[b]	4748±478[a]	8[b]	2178±487[a]	7[b]	5923±399[a]	9[b]	4556±659[a]	9[b]	2044±807[a]	10[b]	2047±496[a]	7[b]
100 000 *g* supernatant	31±7[a]	0.8[b]	33±8[a]	0.3[b]	28±7[a]	0.4[b]	40±12[a]	0.3[b]	46±5[a]	0.4[b]	14±4[a]	0.4[b]	22±12[a]	0.5[b]

A549 cells were homogenized with a Polytron homogenizer, and the homogenate was fractionated by differential centrifugation as described previously [23]. The aliquots of each subcellular fraction were assayed for the protein contents and the CER species contents as described in Experimental.

[a] Mean±SD of triplicate measurements.

[b] Mean of three determinations.

Table 4
Subcellular localization of each CER content in HepG2 cells

Fraction	d18:1-C16:0-CER (pmol/mg protein)	Yield (%)	d18:1-C18:0-CER (pmol/mg protein)	Yield (%)	d18:1-C20:1-CER (pmol/mg protein)	Yield (%)	d18:1-C20:0-CER (pmol/mg protein)	Yield (%)	d18:1-C22:1-CER (pmol/mg protein)	Yield (%)	d18:1-C22:0-CER (pmol/mg protein)	Yield (%)	d18:1-C24:1-CER (pmol/mg protein)	Yield (%)
Homogenate	546±163[a]	100[b]	1941±551[a]	100[b]	1120±301[a]	100[b]	1826±251[a]	100[b]	2993±621[a]	100[b]	1568±439[a]	100[b]	1021±257[a]	100[b]
Nuclear envelope	1006±259[a]	16[b]	2581±631[a]	12[b]	1704±553[a]	13[b]	2947±292[a]	14[b]	4951±568[a]	13[b]	2718±500[a]	16[b]	1666±435[a]	14[b]
7000 *g* pellet	740±151[a]	14[b]	2469±243[a]	14[b]	1665±123[a]	17[b]	2448±180[a]	14[b]	3837±230[a]	14[b]	2025±299[a]	15[b]	1478±241[a]	17[b]
100 000 *g* pellet	835±116[a]	6[b]	3082±427[a]	7[b]	1852±461[a]	7[b]	3059±1109[a]	7[b]	5101±2232[a]	7[b]	2315±799[a]	7[b]	1242±356[a]	5[b]
100 000 *g* supernatant	91±58[a]	5[b]	436±146[a]	5[b]	402±154[a]	9[b]	841±284[a]	11[b]	1478±460[a]	12[b]	529±131[a]	8[b]	280±65[a]	7[b]

HepG2 cells were homogenized with a Potter–Elvehjem PTFE homogenizer, and the homogenate was fractionated by differential centrifugation as described previously [23]. The aliquots of each subcellular fraction were assayed for the protein contents and the CER species contents as described in Experimental.

[a] Mean±SD of triplicate measurements.

[b] Mean of three determinations.

d18:1-C20:0-CER/d18:1-C22:1-CER, d17:1-C21:0-CER/d17:1-C23:1-CER, d20:1-C18:0-CER/d20:1-C20:1-CER and d19:1-C19:0-CER/d19:1-C21:1-CER; and fraction D would likely consists d18:1-C22:0-CER/d18:1-C24:1-CER, d17:1-C23:0-CER/d17:1-C25:1-CER, d20:1-C20:0-CER/d20:1-C22:1-CER and d19:1-C21:0-CER/d19:1-C23:1-CER.

Each CER content in each subcellular fraction obtained on sucrose density gradient centrifugation of HepG2 or A549 cells is shown in Tables 3 and 4. The 7000 *g* pellet fraction of HepG2/A549 cells likely contained a number of cell membranes, lysosomes, mitochondria and heavy-microsomes as described previously [23]. The 100 000 *g* pellet fraction of HepG2/A549 cells likely contained a number of cell membranes and light-microsomes as described previously [23]. The nuclear envelope fraction of HepG2/A549 cells likely contained a number of nuclear envelopes and DNA as described previously [23]. Although CER species contents per mg protein were high in the nuclear envelope, the 7000 *g* pellet fractions and 100 000 *g* pellet fractions from A549/HepG2 cells, a large portion of the CER species in A549 cells was concentrated in the nuclear envelope fraction (Tables 3 and 4). In HepG2 cells, a large portion of the CER species was concentrated in the nuclear envelope fraction or 7000 *g* pellet fractions (Table 4). The 7000 *g* pellet fraction contained the nuclear envelope fragments, heavy microsomes, cell membranes and lysosome with mitochondria [23] and thus it was thought that CER synthesis was localized at the cytosolic surface of intact endoplasmic reticulum [25], the CERs species were widely distributed in the neighboring nuclear envelope and the CERs acted as important intracellular second messengers in diverse biological processes.

The SIM chromatograms of MNa^+ and MH^+–

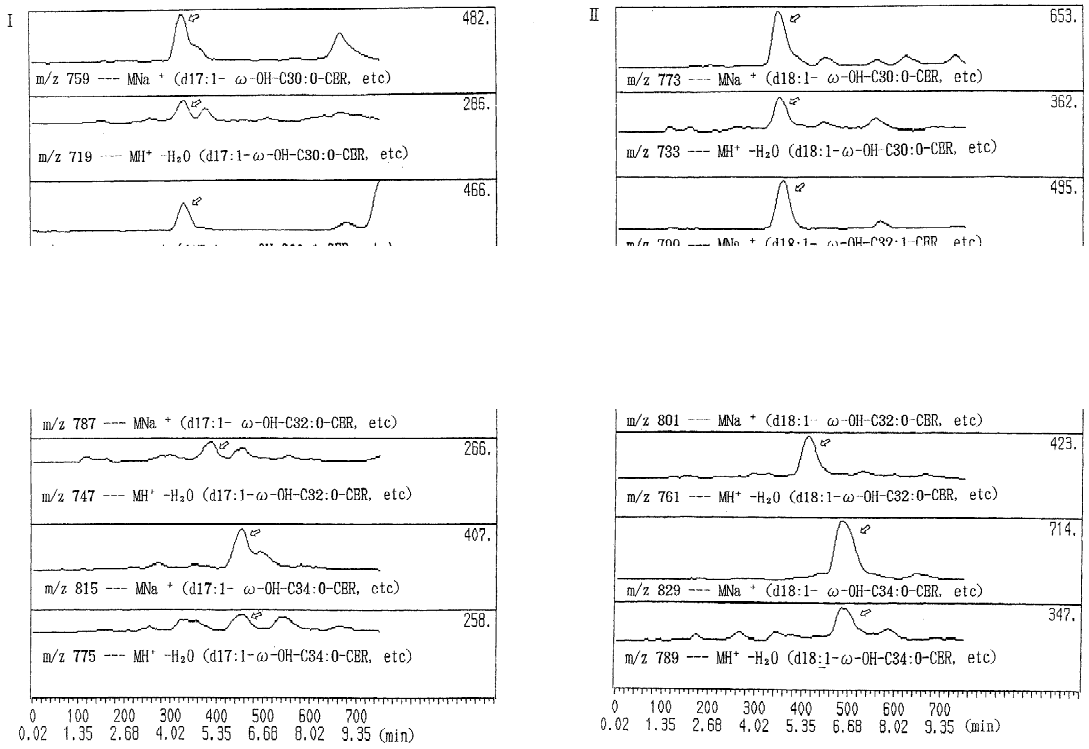

Fig. 6. SIM chromatograms of MNa^+ and MH^+–H_2O ions of ω-hydroxyacyl-CERs from total CERs of pig stratum corneum. A 0.05 *M* ammonium formate–methanol solution was used as the mobile phase. Other conditions were as described in Experimental. Filament off condition. The number in the upper right-hand corner of each chromatogram is the ion count. (I) d17:1-ω-hydroxyacyl-CERs; (II) d18:1-ω-hydroxyacyl-CERs. ω-Hydroxyacyl-CERs indicated with downward arrows.

H_2O ions of ω-hydroxyacyl-CERs from total CERs of pig stratum corneum are shown in Fig. 6I and II. The peaks (indicated with a downward arrow) of $MNa^+/MH^+–H_2O$ ions corresponding to d17:1 (or d18:1)-ω-hydroxy-C30:0-CER, d17:1 (or d18:1)-ω-hydroxy-C32:1-CER, d17:1 (or d18:1)-ω-hydroxy-C32:0-CER, d17:1 (or d18:1)-ω-hydroxy-C34:0-CER were detected as shown in Fig. 6I and II. Since these peaks were not detected in the SIM chromatograms corresponding to each MNa^+ and $MH^+–H_2O$ ion in total CERs from pig stratum corneum, the peaks indicated with downward arrows would not be due to the ions corresponding to phytosphingosine-CERs or d17:1 (or d18:1)-α-hydroxy-CERs in total CERs from pig stratum corneum.

Since there was a low-rate of elimination as water of the hydroxyl group introduced at the ω-position of fatty acid in the TSP-interface as described previously [26,27], the preponderance of MNa^+ ions compared with the $MH^+–H_2O$ ions was consistent. On the other hand, although the m/z value of ω-hydroxyacyl-CER was the same as that of the corresponding α-hydroxyacyl-CER, a preponderance of $MH^+–H_2O$ ions based on the elimination of the hydroxyl group introduced at the α-position of the acyl-portion compared with the MNa^+ ion was detected in TSP-interface-MS analysis as shown in Fig. 1B. In addition, the retention time of ω-hydroxyacyl-CER on the HPLC was shorter than that of the corresponding α-hydroxyacyl-CER (data not shown). Consequently, it is possible to achieve fractional determination of ω-hydroxyacyl-CER and the corresponding α-hydroxyacyl-CER using HPLC–TSP-MS analysis. In APCI- and ESI-MS of CERs, significant information regarding the position of the hydroxyl group was not described [17–21].

Though MS–MS analysis such as APCI-MS–MS or ESI-MS–MS analysis yielded high sensitivity and accuracy compared with single MS analysis such as TSP-MS, APCI-MS or ESI-MS analysis, the characteristic fragmentations regarding the position of the hydroxyl group in CERs in TSP-MS analysis were utilized for fractional determination.

References

[1] Y.A. Hannun, J. Biol. Chem. 269 (1994) 3125.
[2] S. Jayadev, B. Liu, A.F. Bielawska, J.Y. Lee, F. Nazaire, M.Y. Pushkareva, L.M. Obeid, Y.A. Hannun, J. Biol. Chem. 270 (1995) 2047.
[3] K. Yokohama, H. Nojiri, M. Suzuki, M. Sekata, A. Suzuki, S. Nojima, FEBS Lett. 368 (1995) 477.
[4] L. Riboni, A. Prinetti, R. Bassi, A. Caminiti, G. Tettamanti, J. Biol. Chem. 270 (1995) 26868.
[5] M.E. Venable, J.Y. Lee, M.J. Smyth, A. Bielawska, L.M. Obeid, J. Biol. Chem. 270 (1995) 30701.
[6] L.A. Pena, Z. Fuks, R. Kolesnick, Biochem. Pharmacol. 53 (1997) 615.
[7] P.P. Van Veldhoven, W.R. Bishop, D.A. Yurivich, R.M. Bell, Biochem. Mol. Biol. Int. 36 (1995) 21.
[8] J.D. Watts, M. Gu, A.J. Polverino, S.D. Patterson, R. Aebersold, Proc. Natl. Acad. Sci. USA 94 (1997) 7292.
[9] S. Motta, M. Monti, S. Sesana, L. Mellesi, R. Ghidoni, R. Caputo, Arch. Dermatol. 130 (1994) 452.
[10] N. Andrieu, R. Salvayre, J.P. Jaffrezou, T. Levade, J. Biol. Chem. 270 (1995) 24518.
[11] E.R. Smith, A.H.J. Merrill, J. Biol. Chem. 270 (1995) 18749.
[12] A.D. Tepper, J.G. Cock, E. de Vries, J. Borst, W.J. van Blitterswijk, J. Biol. Chem. 272 (1997) 24308.
[13] M. Iwamori, C. Costello, H.W. Moser, J. Lipid Res. 20 (1979) 86.
[14] M. Previati, L. Bertolaso, M. Tramarin, V. Bertagnolo, S. Capitani, Anal. Biochem. 233 (1996) 108.
[15] M. Garzotto, J.M. White, Y. Jiang, D. Ehleiter, W.C. Liao, F.A. Haimovitz, Z. Fuks, R. Kolesnick, Cancer Res. 58 (1998) 2260.
[16] M. Yano, E. Kishida, Y. Muneyuki, Y. Masuzawa, J. Lipid Res. 39 (1998) 2091.
[17] L.H. Couch, M.I. Churchwell, D.R. Doerge, W.H. Tolleson, P.C. Howard, Rapid Commun. Mass Spectrom. 11 (1997) 504.
[18] M. Gu, J.L. Kerwin, J.D. Watts, R. Aebersold, Anal. Biochem. 244 (1997) 347.
[19] N. Mano, Y. Oda, K. Yamada, N. Asakawa, K. Katayama, Anal. Biochem. 244 (1997) 291.
[20] G. Liebisch, W. Drobnik, M. Reil, B. Trumbach, R. Arnecke, B. Olgemoller, A. Roscher, G. Schmitz, J. Lipid Res. 40 (1999) 1539.
[21] Y. Yamada, K. Kajiwara, M. Yano, E. Kishida, Y. Masuzawa, S. Kojo, Biochim. Biophys. Acta 1532 (2001) 115.
[22] P.W. Wertz, D.T. Downing, Biochim. Biophys. Acta 917 (1987) 108.
[23] M. Yamane, A. Abe, J. Biochem. 128 (2000) 827.
[24] P.W. Wertz, D.C. Swartzendruber, K.C. Madison, D.T. Downing, J. Invest. Dermatol. 89 (1987) 419.
[25] K. Hirschberg, J. Rodger, A.H. Futerman, Biochem. J. 290 (1993) 751.
[26] M. Yamane, A. Abe, M. Nakajima, J. Chromatogr. B 662 (1994) 91.
[27] S. Shimizu, M. Yamane, A. Abe, M. Nakajima, H. Sugiura, M. Miyaoka, T. Saitoh, Biochim. Biophys. Acta 1256 (1995) 293.
[28] M. Fillet, J.-C. VanHeugen, A.-C. Servais, J. DeGraeve, J. Crommen, J. Chromatogr. A 949 (2002) 225.